

## ELECTROCHEMICAL IMPEDANCE SPECTROSCOPY STUDY OF ELECTRON TRANSFER AT POLY(3,4-ETHYLENEDIOXYTHIOPHENE) CONTAINING GOLD NANOPARTICLES COATING

Stelian LUPU

*Department of Analytical Chemistry and Instrumental Analysis,  
Faculty of Applied Chemistry and Materials Science, University Politehnica of Bucharest,  
Polizu Gheorghe 1-3, 011061 Bucharest, Romania; e-mail: stelianl@yahoo.com*

Received May 25, 2011

Accepted June 19, 2011

Published online December 2, 2011

Electrochemical impedance spectroscopy (EIS) was used for characterization of electron transfer in various redox probes, such as the redox couple ferrocyanide-ferricyanide, ferrocene, ferrocenemethanol, and the poly(3,4-ethylenedioxothiophene) (PEDOT) conducting polymer containing gold nanoparticles. The PEDOT coating was deposited onto platinum (Pt) and glassy carbon (GC) electrodes by galvanostatic electrochemical polymerization from an aqueous solution containing  $10^{-2}$  M EDOT and  $10^{-1}$  M LiClO<sub>4</sub> as supporting electrolyte. The PEDOT-Au nanoparticles composite coating was prepared by droplet deposition of Au nanoparticles on top of the Pt/PEDOT and GC/PEDOT modified electrodes. The pure PEDOT and PEDOT-Au nanoparticles composite coatings were investigated using EIS and cyclic voltammetry (CV) in  $10^{-1}$  M LiClO<sub>4</sub> solution containing various redox probes. The impedance spectra were recorded at the formal redox potential of the redox probes. The charge transfer resistance ( $R_{ct}$ ), solution resistance ( $R_s$ ), exchange current density ( $i_0$ ), standard rate constant ( $k_0$ ), and double-layer capacitance ( $C_{dl}$ ) were calculated from the EIS data.

**Keywords:** Electrochemical impedance spectroscopy; Cyclic voltammetry; Modified electrode; Conducting polymer; Au nanoparticles; Electrochemistry; Nanoparticles; Polymers.

Metal-nanoparticles based composite materials have attracted a great deal of interest in the last decade due to their unique electrochemical, optical, electronic and catalytic properties, and their potential use in electrochemical sensors and biosensors<sup>1-8</sup>. Noble metal nanoparticles (NPs) were incorporated into conducting polymers in order to improve their analytical performances<sup>9</sup>. Various chemical<sup>10,11</sup> and electrochemical<sup>12-19</sup> methods have been developed for ex situ or in situ NPs preparation. The incorporation of NPs in conducting polymers has been achieved by self assembly of chemically pre-synthesized NPs onto SAM<sup>20</sup>, electrochemical deposition of chemically pre-synthesized NPs onto polymer films<sup>21</sup>, electrochemical poly-

merization of the appropriate monomer in the presence of chemically pre-synthesized NPs<sup>9</sup>, and layer-by-layer intercalation of the inorganic NPs into conducting polymer composite coatings<sup>6,22</sup>.

Among various conducting polymers, 3,4-ethylenedioxothiophene (EDOT) has been quite extensively studied for NPs incorporation into polymeric films<sup>23,24</sup>, mainly for its excellent stability and the possibility to prepare the corresponding PEDOT polymer matrix through electrochemical polymerization of the EDOT monomer in aqueous solution<sup>25-32</sup>.

In this work, the electrochemical behavior of inorganic-organic composite materials consisting of poly(3,4-ethylenedioxothiophene) (PEDOT) conducting polymer and Au nanoparticles was investigated using electrochemical impedance spectroscopy (EIS) and cyclic voltammetry (CV) methods in aqueous solution containing various redox probes. The electron transfer between the redox probes, such as the redox couple ferrocyanide-ferricyanide, and the PEDOT-Au nanoparticles inorganic-organic composite materials deposited onto Pt and GC electrodes was studied in terms of kinetic parameters and electrochemical properties, i.e., the charge transfer resistance ( $R_{ct}$ ), solution resistance ( $R_s$ ), exchange current density ( $i_0$ ), standard rate constant ( $k_0$ ), and double-layer capacitance ( $C_{dl}$ ). The PEDOT organic layers were deposited onto Pt and GC electrodes by galvanostatic electrochemical polymerization from an aqueous solution containing  $10^{-2}$  M EDOT and  $10^{-1}$  M LiClO<sub>4</sub> as supporting electrolyte. The PEDOT-Au nanoparticles composite coatings were prepared by two methods: (i) droplet deposition of Au nanoparticles on top of the Pt/PEDOT modified electrodes; (ii) electrochemical polymerization of EDOT in the presence of Au nanoparticles. The Pt/PEDOT, GC/PEDOT, GC/PEDOT-Au nanoparticles, and Pt/PEDOT-Au nanoparticles modified electrodes were investigated using EIS and CV in  $10^{-1}$  M LiClO<sub>4</sub> containing ferrocyanide-ferricyanide as the redox probe. The impedance spectra were recorded at the formal redox potential of the redox probe. The charge transfer resistance ( $R_{ct}$ ), solution resistance ( $R_s$ ), exchange current density ( $i_0$ ), standard rate constant ( $k_0$ ), and double-layer capacitance ( $C_{dl}$ ) were calculated from the EIS data.

### *Theory and Principles of EIS Measurements*

The kinetics of the electron transfer between the soluble redox probe and the polymer/polymer-Au nanoparticles coatings was analyzed using the Butler-Volmer equation<sup>33</sup>. The exchange current  $i_0$  is given by the equation

$$i_0 = nFAk_0C_{\text{Ox}} \exp\left[-\alpha nF(E_{\text{dc}} - E^{0'})/RT\right] = \\ = nFAk_0C_{\text{Red}} \exp\left[(1-\alpha)nF(E_{\text{dc}} - E^{0'})/RT\right] \quad (1)$$

where  $A$  is the area of the electrode,  $k_0$  is the standard rate constant,  $C_{\text{Ox}}$  and  $C_{\text{Red}}$  are the bulk concentrations of the oxidized and reduced forms of the redox couple in solution, respectively,  $E_{\text{dc}}$  is the equilibrium dc potential of the electrode,  $E^{0'}$  is the formal potential of the redox couple in the solution, and the other symbols have their usual electrochemical meaning. The EIS measurements were performed under such experimental conditions that is  $E_{\text{dc}} = E^{0'}$  and  $C_{\text{Ox}} = C_{\text{Red}} = C$ . In this case, Eq. (1) reduces to

$$i_0 = nFAk_0C. \quad (2)$$

The charge transfer resistance  $R_{\text{ct}}$  for the electron transfer process (at small overpotentials) is

$$R_{\text{ct}} = RT/nFi_0. \quad (3)$$

From Eqs (2) and (3) one can obtain the expression of  $k_0$

$$k_0 = RT/n^2F^2R_{\text{ct}}AC. \quad (4)$$

## EXPERIMENTAL

### Materials

$\text{K}_4[\text{Fe}(\text{CN})_6]$  (Merck),  $\text{K}_3[\text{Fe}(\text{CN})_6]$  (Merck),  $\text{LiClO}_4$  (Merck), ferrocene (Merck), ferrocene-methanol (Aldrich), acetonitrile (Merck), and 3,4-ethylenedioxythiophene (EDOT; Aldrich) were used without further purification. Deionised water Millipore (18  $\text{M}\Omega \text{ cm}$ ) was always used to prepare aqueous solutions. Because the mixture of  $\text{K}_4[\text{Fe}(\text{CN})_6]/\text{K}_3[\text{Fe}(\text{CN})_6]$  tends to form Prussian Blue adsorbing to the electrode surface, all the solutions were freshly prepared.

### Apparatus

The electrochemical polymerizations and characterization experiments were carried out with an Autolab PGSTAT 30 potentiostat/galvanostat (Eco Chemie B.V., The Netherlands) coupled to a PC running the GPES, using a single-compartment, three-electrode cell, at room temperature. The impedance spectra were recorded using the Autolab frequency response analyzer system AUT20.FRA2-AUTOLAB (Eco Chemie B.V., The Netherlands). A 3-mm diameter Pt disk electrode (Metrohm) and/or a 2-mm diameter GC disk electrode (home made) were the working electrodes, a silver-silver chloride/3 M KCl electrode ( $\text{Ag}/\text{AgCl}$ , Amel) was the refer-

ence electrode, and a Pt wire (Metrohm), twisted around the working electrode, was the auxiliary electrode. The electrochemical measurements were performed inside a Faraday cage. Before each electrochemical test, the surface of the working electrode was polished subsequently with 1, 0.3 and 0.05  $\mu\text{m}$  alumina powder to a mirror finish, rinsed then with deionised water and ultrasonicated for 5 min. All the solutions used for the electrochemical measurements were bubbled with Ar for 10 min and an Ar flow was maintained over the solutions during the experiments. The impedance spectra were recorded in the frequency range 0.1–10 kHz using a sinusoidal excitation signal (single sine) with excitation amplitude ( $\Delta E_{\text{ac}}$ ) of 5 mV. The electrochemical properties of the coatings were checked using CV before and after the EIS measurements. The impedance spectra were recorded at the open circuit potential (i.e.  $E^{\text{o}} = 0.20$  V vs Ag|AgCl in the case of ferrocyanide-ferricyanide redox couple) in  $10^{-1}$  M LiClO<sub>4</sub> aqueous solution containing various redox probes, such as  $[\text{Fe}(\text{CN})_6]^{3-4-}$ , with equal concentrations of the oxidized and reduced form, i.e.  $C_{\text{Ox}} = C_{\text{Red}} = C = 1$  mmol l<sup>-1</sup>.

### Preparation Procedures of PEDOT and PEDOT-Au Nanoparticles Coatings

The PEDOT coating was deposited onto Pt electrodes by galvanostatic electrochemical polymerization from an aqueous solution containing  $10^{-2}$  M EDOT and  $10^{-1}$  M LiClO<sub>4</sub> as supporting electrolyte. A constant current of 28.3  $\mu\text{A}$  was applied for 160 s to produce a polymerization charge of  $6.4 \times 10^{-2}$  C cm<sup>-2</sup> for the 3-mm Pt disk electrode, while a constant current of 12.6  $\mu\text{A}$  was applied at various times ranging from 20 to 160 s, in the case of the 2-mm GC disk electrode. A polymerization charge of  $6.4 \times 10^{-2}$  C cm<sup>-2</sup> corresponds to PEDOT film thickness of approximately 0.5  $\mu\text{m}$ , assuming 2.25 electrons/monomer and a film density of 1 g cm<sup>-3</sup> (ref.<sup>34</sup>). The PEDOT-Au nanoparticles composite coatings were prepared by droplet evaporation of 11  $\mu\text{l}$  (Pt electrode) or 7  $\mu\text{l}$  (GC electrode) of Au-citrate nanoparticles solution on the top of the PEDOT-modified electrode. Another preparation procedure consists of the co-deposition of Au nanoparticles during the electrochemical polymerization of EDOT in an aqueous solution. After the formation of the composite PEDOT-Au nanoparticles coating, the modified electrode was rinsed with deionised water and then immersed in  $10^{-1}$  M LiClO<sub>4</sub> aqueous solution where it was characterised using CV and EIS in the absence and presence of the redox probe, respectively.

## RESULTS AND DISCUSSION

The  $R_{\text{ct}}$  value is a direct measure of the standard rate constant  $k_0$  that is related to  $k_f$  and  $k_b$  of the electrochemical reaction through Eq. (4). The values of  $i_0$  and  $k_0$  can be calculated using Eqs (3) and (4), respectively, when  $R_{\text{ct}}$  is obtained by fitting the experimental EIS data using the FRA2 software of the potentiostat/galvanostat Autolab 30. The software makes use of various electric equivalent circuits (EECs). For this purpose we used an EEC consisting of the solution resistance; the charge transfer resistance due to electron transfer at the polymer/solution interface; the infinite-length Warburg diffusion impedance due to diffusion of the redox couple in the solution; the electronic bulk (redox) capacitance of the polymer film; the finite-length Warburg diffusion impedance due to diffusion of charge-

compensating counterions in the polymer film. This EEC is similar to those reported in the literature<sup>34</sup>. In case of high impedance values, the charge transfer resistance and the solution resistance were determined using a graphical method, i.e., from the  $Z'$  vs  $-\omega Z''$  plot<sup>35</sup>.

The incorporation of the redox couple into the pure PEDOT matrix may take place during the EIS measurements. Before and after the EIS measurements, the cyclic voltammograms of the modified electrodes were recorded in  $10^{-1}$  M LiClO<sub>4</sub>. The appearance of small peaks suggests that the incorporation of the redox probe takes place during the EIS measurements. In order to assess the quantity of the redox probe incorporated into the PEDOT matrix, the surface concentration  $\Gamma$  was calculated using Eq. (5), after proper subtracting of the blank voltammogram

$$\Gamma = Q/nFA \quad (5)$$

where  $Q$  is the charge calculated from the corresponding CV peak. The electrochemical properties of the PEDOT and PEDOT-Au nanoparticles were first checked in the absence of the redox probe in the electrolyte solution. Furthermore, there is no incorporation of the redox probe inside the PEDOT-Au nanoparticles composite coating, unlike as previously observed in the case of pure PEDOT-only coating<sup>34</sup>. This behavior may be due to the presence of the Au nanoparticles in the pores of the PEDOT matrix.

The influence of the measurement sequence on the PEDOT-Au nanoparticles coatings was also studied. The sequence of the measurements, i.e., CV followed by EIS measurements, does not influence the electrochemical properties of the coating. There is only a very small decrease in the current, which is limited to the expected experimental error. The stability of the composite coatings was very good.

The co-deposition of Au nanoparticles along with the electrochemical polymerization of EDOT failed due to the precipitation of nanoparticles in the presence of the supporting electrolyte and as a result of a chemical reaction with the monomer. The kinetic parameters, such as charge transfer resistance, exchange current density, standard rate constant, have values similar to those reported in the literature for the PEDOT-only coating deposited onto Pt electrodes<sup>36–38</sup>.

### *Electrochemical Properties of PEDOT Coating*

Pt and GC electrodes were used as the substrate for the PEDOT deposition in this work. Before the PEDOT deposition, the naked electrodes were char-

acterized by EIS. Figure 1 shows the EIS spectra recorded at the Pt and GC electrodes in 1 mm  $[\text{Fe}(\text{CN})_6]^{3-4-}$ , 10<sup>-1</sup> M LiClO<sub>4</sub> aqueous solution at the equilibrium potential of the redox couple. The shape of the EIS spectra is the classical one, corresponding to a Randles circuit. The semi-circle located at high frequencies is related to the charge transfer resistance, which has a higher value for the naked Pt electrode compared to the naked GC electrode; this suggests a more facile electron transfer at the GC electrode. However, the solution resistance that includes the electrical resistance of the GC electrode, is always higher than that of the Pt electrode. This behavior is due to the fact that the GC electrodes were prepared in the laboratory, making the electrical contact through a copper wire. The GC electrode surface is prone to adsorption of the redox probe during cyclic voltammetry and electrochemical impedance measurements, and this behavior may also explain such a difference in the  $R_{\text{ct}}$  values.

The EIS spectra were then recorded for PEDOT film at an ac frequency varying from 0.1 Hz to 10 kHz in the electrode potential region from -0.8 to 0.5 V, in the 10<sup>-1</sup> M LiClO<sub>4</sub> solution. The Nyquist plots of impedance spectra obtained for PEDOT film exhibit a shape typical for conducting polythiophenes, not shown here for this reason. However, a brief discussion of these spectra is provided in order to explain the impedance spectra

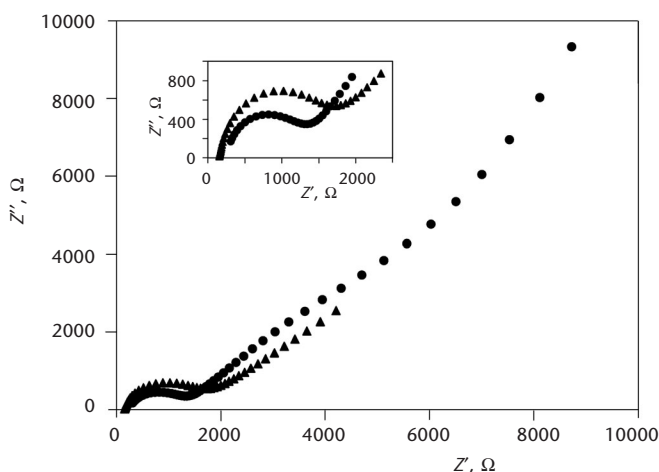


FIG. 1  
Nyquist plots of the impedance spectra recorded at the Pt (●) and GC (▲) electrodes in 1 mm  $[\text{Fe}(\text{CN})_6]^{3-4-}$ , 10<sup>-1</sup> M LiClO<sub>4</sub> (aq.) at the equilibrium potential for ac frequencies ranging from 0.1 Hz to 10 kHz. Inset: in zoom of the high frequency region

recorded in the presence of a redox probe. There are three characteristic parts of the EIS spectra, recorded at the Pt/PEDOT modified electrode in the supporting electrolyte, in the Nyquist plots: a semi-circle located in the range of high frequencies, a short transition region similar to the Warburg type, and a linear capacitive response at low frequencies. Depending on the dc voltages the shape of the EIS spectra displays two patterns: at high frequencies a semi-circle is obtained, which is related to the interfacial processes. The charge transfer resistance is potential-dependent, decreasing as the dc potential reaches more positive values. The low-frequency region of these Nyquist plots indicates the capacitive behavior related to the film-charging mechanism.

The electrochemical impedance spectra of pure PEDOT coatings deposited on the Pt and GC electrodes were also recorded in the presence of the redox couple. The high frequency region of these spectra is dominated by the interfacial electron transfer resulting in a well defined semi-circle in the corresponding Nyquist plot. Unlike the Pt/PEDOT modified electrode, the semi-circle is less defined for the GC/PEDOT modified electrode (Fig. 2). The low-frequency region is dominated by the diffusion of both the electroactive species of the redox couple and the counterions necessary to maintain the electroneutrality inside the PEDOT film.

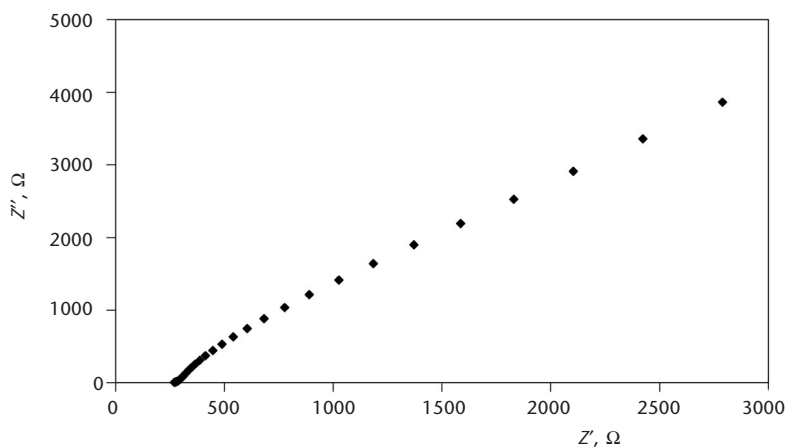


FIG. 2

Nyquist plot of the impedance spectrum recorded at the GC/PEDOT modified electrode in  $1 \text{ mM } K_3[Fe(CN)_6]/K_4[Fe(CN)_6]$ ,  $10^{-1} \text{ M LiClO}_4$  (aq.) at different dc potentials for ac frequencies ranging from 0.1 Hz to 10 kHz

During the EIS measurements the incorporation of the soluble redox couple inside the PEDOT film takes place in some cases. This behavior was also reported for PEDOT films and resulted in an irregular dependence of kinetic parameters on the redox probe concentration<sup>36,37</sup>. For these reasons a lower redox probe concentration, i.e., 1 mmol l<sup>-1</sup>, was chosen and the GC/PEDOT modified electrodes were further investigated, making comparison with the Pt/PEDOT modified electrode to highlight important different electrochemical features. The amounts of the incorporated redox species were calculated according to Eq. (5). A value of  $1.22 \times 10^{-9}$  mol cm<sup>-2</sup> was calculated for the PEDOT-only coating deposited on the GC electrode.

#### *Electrochemical Properties of Au-Nanoparticles Doped PEDOT Coating*

The EIS spectra were also recorded for the Au-nanoparticles doped PEDOT films at an ac frequency varying from 0.1 Hz to 100 kHz at the equilibrium potential of the redox couple in 10<sup>-1</sup> M LiClO<sub>4</sub> aqueous solution (Fig. 3).

The Nyquist plots of impedance spectra obtained for the Au-nanoparticles doped PEDOT film exhibit the shape typical for pure PEDOT coatings. However, there is a difference in the high frequency region of the impedance spectra seen as the appearance of a well defined semi-circle, which at-

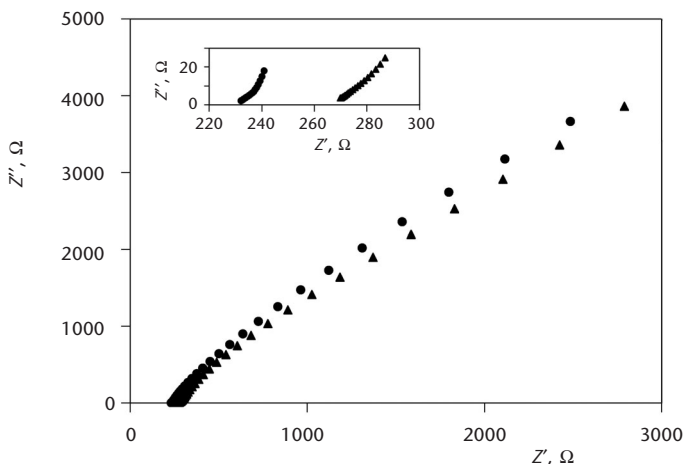


FIG. 3

Nyquist plots of the impedance spectra recorded at the GC/PEDOT (▲) and GC/PEDOT-Au nanoparticles (●) modified electrodes in 1 mm K<sub>3</sub>[Fe(CN)<sub>6</sub>]/K<sub>4</sub>[Fe(CN)<sub>6</sub>], 10<sup>-1</sup> M LiClO<sub>4</sub> (aq.) at the equilibrium potential for ac frequencies ranging from 0.1 Hz to 10 kHz. Inset: in zoom of the high frequency region

tests the improved electron transfer capacity of the Au-nanoparticles doped PEDOT coating with respect to the pure PEDOT one. The presence of the Au nanoparticles inside the PEDOT matrix reduces the incorporation of the soluble redox couple into the organic polymer layer. The impedance spectra were also recorded for various Au-nanoparticles doped PEDOT coatings and the obtained electrochemical parameters are presented in Table I.

The kinetic parameters such as charge transfer resistance, exchange current density, and standard rate constant, have values similar to those reported in the literature for a PEDOT-only coating deposited onto Pt electrodes. The composite coatings PEDOT-Au nanoparticles showed the smallest values for  $R_{ct}$  in comparison with PEDOT-only coatings. These findings are well supported by the data represented as Bode plots in Fig. 4.

The polymerization times used for the electrochemical deposition of a PEDOT layer onto the GC electrode surface were 20, 40, 80, and 160 s. These polymerization times correspond to polymerization charges 8, 16, 32, and 64  $\text{mC cm}^{-2}$ , respectively. The estimated thicknesses of the corresponding PEDOT coatings were in the range from 0.06 to 0.50  $\mu\text{m}$ , assuming 2.25 electrons/monomer and a film density of 1  $\text{g cm}^{-3}$  (ref.<sup>34</sup>). There is no linear dependence between the charge transfer resistance and the polymer-

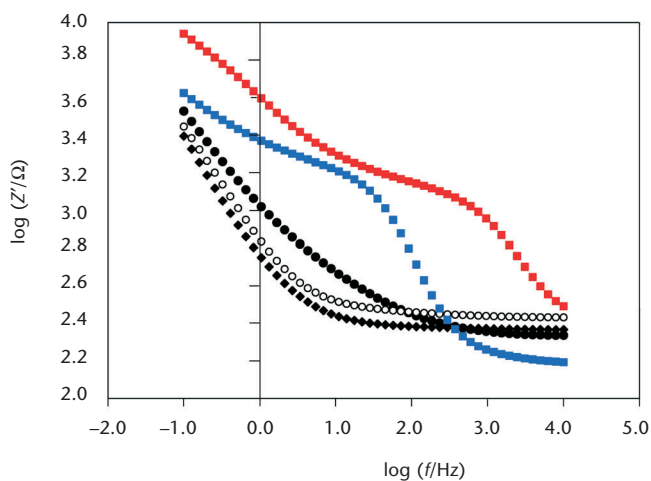


FIG. 4

Bode plots for the naked Pt (blue) and GC (red) electrodes, and the GC electrodes modified with the pure PEDOT ( $\circ$ , 160 s) and PEDOT-Au nanoparticles ( $\blacklozenge$ , 20 s;  $\bullet$ , 160 s) composite coatings. The experimental conditions as in Fig. 3

ization charge (Fig. 5). However, this should not be considered as a poor reproducibility of the pure PEDOT coatings obtained by electrochemical polymerization for different deposition times, but rather as a consequence of the incorporation of pre-synthesized Au nanoparticles inside the PEDOT matrix. These results suggest that there is an optimum deposition time of the PEDOT coating for which the lowest  $R_{ct}$  value is obtained. Hence, a composite coating capable of a faster electron transfer kinetics could be prepared in this manner. This behavior can therefore be ascribed to the complexity of the composite coatings, the morphology of such materials then being strongly dependent on the experimental conditions and the electrode substrate.

TABLE I  
Kinetic parameters calculated from EIS spectra and CV measurements

| Electrode (polymerization charge)  | $R_{ct}$ , $\Omega^a$ | $R_s$ , $\Omega^b$ | $i_0$ , $A\text{ cm}^{-2}c$ | $k_0$ , $\text{cm s}^{-1}d$ | $C_{dl}$ , $\mu\text{F cm}^{-2}e$ |
|--|-----------------------|--------------------|-----------------------------|-----------------------------|-----------------------------------|
| Pt in 1 mM ferro-ferricyanide, 0.1 M LiClO <sub>4</sub>  | 1738                  | 152                | 2.10E-04                    | 2.20E-03                    | 68                                |
| Pt in 1 mM ferro-ferricyanide, 0.1 M LiClO <sub>4</sub><br>(after electrochemical cleaning)                    | 866                   | 162                | 4.20E-04                    | 4.35E-03                    | 29                                |
| GC in 0.1 M LiClO <sub>4</sub> ( $E_{dc} = 0.200$ V)   | 643                   | 271                | —                           | —                           | 7                                 |
| Pt/PEDOT (64 mC cm <sup>-2</sup> ) in 0.1 M LiClO <sub>4</sub><br>( $E_{dc} = 0.200$ V)                        | 5                     | 160                | —                           | —                           | 727                               |
| Pt/PEDOT (64 mC cm <sup>-2</sup> ) in 1 mM<br>ferro-ferricyanide, 0.1 M LiClO <sub>4</sub>                     | 7                     | 174                | 5.19E-02                    | 5.38E-01                    | 1014                              |
| GC/PEDOT (16 mC cm <sup>-2</sup> ) in 0.1 M LiClO <sub>4</sub>   | 8                     | 348                | —                           | —                           | 1346                              |
| GC/PEDOT-Au nanopart-citrate (16 mC cm <sup>-2</sup> )<br>in 1 mM ferro-ferricyanide, 0.1 M LiClO <sub>4</sub> | 14                    | 330                | 5.84E-02                    | 6.05E-01                    | 2330                              |
| GC/PEDOT-Au nanopart-citrate (16 mC cm <sup>-2</sup> )<br>in 0.1 M LiClO <sub>4</sub>                          | 7                     | 340                | —                           | —                           | 968                               |
| GC/PEDOT (32 mC cm <sup>-2</sup> ) in 0.1 M LiClO <sub>4</sub>   | 5                     | 431                | —                           | —                           | 706                               |
| GC/PEDOT (32 mC cm <sup>-2</sup> ) in 1 mM<br>ferro-ferricyanide, 0.1 M LiClO <sub>4</sub>                     | 7                     | 421                | 1.17E-01                    | 1.21                        | 1085                              |
| GC/PEDOT-Au nanopart-citrate (32 mC cm <sup>-2</sup> )<br>in 0.1 M LiClO <sub>4</sub>                          | 15                    | 1332               | —                           | —                           | 592                               |
| GC/PEDOT-Au nanopart-citrate (32 mC cm <sup>-2</sup> )<br>in 1 mM ferro-ferricyanide, 0.1 M LiClO <sub>4</sub> | 8                     | 1286               | 1.02E-01                    | 1.06                        | 270                               |
| GC/PEDOT (64 mC cm <sup>-2</sup> ) in 1 mM<br>ferro-ferricyanide, 0.1 M LiClO <sub>4</sub>                     | 3150                  | —                  | 2.63E-04                    | 2.76E-03                    | —                                 |

<sup>a</sup>  $R_{ct}$ , charge transfer resistance; <sup>b</sup>  $R_s$ , solution resistance; <sup>c</sup>  $i_0$ , exchange current density;

<sup>d</sup>  $k_0$ , standard rate constant; <sup>e</sup>  $C_{dl}$ , double layer capacitance.

The kinetics of the electron transfer between PEDOT-Au nanoparticles composite coatings and other redox probes, such as ferrocene and ferrocene-methanol, were also investigated in both aqueous and organic media. A stronger incorporation of the redox probe inside the PEDOT based composite coatings was observed. Another composite coating obtained by electrochemical polymerization of the EDOT monomer in aqueous solution in the presence of potassium ferricyanide at a concentration level of  $10^{-1}$  mol l<sup>-1</sup> was investigated. The resulting composite coating contained the PEDOT matrix fully doped with ferro-ferricyanide ions, but during the electrochemical impedance measurements performed on this coating both the release and the incorporation of the redox probe from the solution were also observed. Therefore, the results presented above can be considered as very accurate since only one coating was affected by the incorporation of the redox probe in the pure PEDOT coating, while no such effect was observed for PEDOT-Au nanoparticles composite coatings, clearly indicating that these composite coating are worthy to investigate.

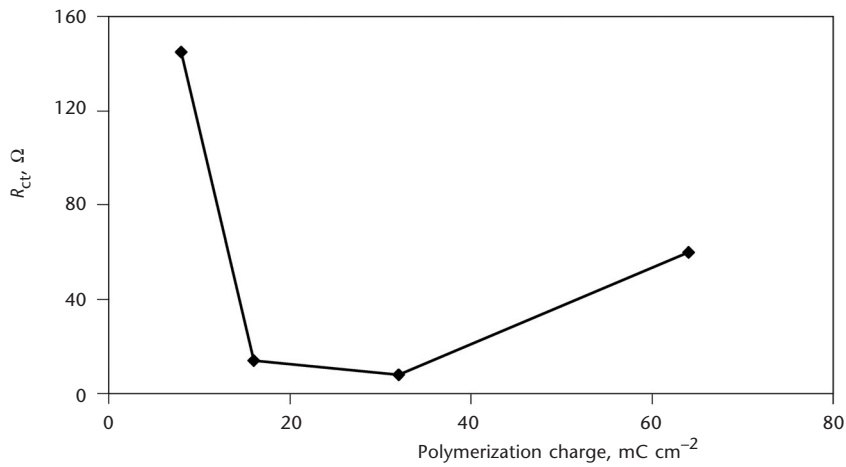


FIG. 5  
Dependence of the charge transfer resistance on the polymerization charge used for the electrodeposition of the PEDOT coating on the GC electrode surface

## CONCLUSIONS

Electrochemical properties of the organic-inorganic composite materials were investigated in the presence of various redox probes as well as in pure supporting electrolyte solution with no added redox probe. Kinetic parameters for the electron transfer between the redox probe and the inor-

ganic-organic composite materials were calculated using electrochemical impedance spectroscopy and cyclic voltammetry methods. The charge transfer resistance of the bare Pt electrode is higher with respect to that observed for the GC electrode, which suggests a more facile electron transfer at the latter. The GC electrode surface is prone to the adsorption of the redox probe during cyclic voltammetry and electrochemical impedance measurements; behavior may also explain such a difference for  $R_{ct}$  values. Unlike the pure PEDOT-only coatings, the composite PEDOT-Au nanoparticles coatings revealed no incorporation of the redox probe, due to the blocking effect and charge of the Au nanoparticles. The kinetic parameters such as charge transfer resistance, exchange current density, standard rate constant, have values similar to those reported in the literature for the PEDOT-only coating deposited onto Pt electrodes<sup>36–38</sup>. The composite coatings PEDOT-Au nanoparticles showed the lowest values for  $R_{ct}$  in comparison with the PEDOT-only coatings. The increased conductivity of these composite coatings containing metal nanoparticles can be useful for analytical applications in designing new electrochemical sensors based on materials capable of mediating fast electron transfer reactions.

*Prof. R. Seeber is acknowledged for supporting the stay of S.L. at the University of Modena and Reggio Emilia as a Visiting Professor, which allowed him to carry out the research reported in this article.*

## REFERENCES

1. Wang J.: *Anal. Chim. Acta* **2003**, *500*, 247.
2. Luo X., Morrin A., Killard A. J., Smyth M. R.: *Electroanalysis* **2006**, *18*, 319.
3. Welch C. M., Compton R. G.: *Anal. Bioanal. Chem.* **2006**, *384*, 601.
4. Guo S., Dong S.: *Trends Anal. Chem.* **2009**, *28*, 96.
5. Willner I., Willner B., Katz E.: *Bioelectrochemistry* **2007**, *70*, 2.
6. Zanardi C., Terzi F., Zanfragnini B., Pigani L., Seeber R., Lukkari J., Ääritalo T.: *Sens. Actuators, B* **2010**, *144*, 92.
7. Campbell F. W., Compton R. G.: *Anal. Bioanal. Chem.* **2010**, *396*, 241.
8. Xu S., Tu G., Peng B., Han X.: *Anal. Chim. Acta* **2006**, *570*, 151.
9. Terzi F., Zanardi C., Martina V., Pigani L., Seeber R.: *J. Electroanal. Chem.* **2008**, *619–620*, 75.
10. Christodoulakis K. E., Paliora D., Anastasiadis S. H., Vamvakaki M.: *Top Catal.* **2009**, *52*, 394.
11. Deng Q. Y., Yang B., Wang J. F., Whiteley C. G., Wang X. N.: *Biotechnol. Lett.* **2009**, *31*, 1505.
12. Maillard F., Savinova E. R., Stimming U.: *J. Electroanal. Chem.* **2007**, *599*, 221.
13. Kuo C. W., Sivakumar C., Wen T. C.: *J. Power Sources* **2008**, *185*, 807.

14. Patra S., Munichandraiah N.: *Langmuir* **2009**, *25*, 1732.
15. Zin V., Pollet B. G., Dabalà M.: *Electrochim. Acta* **2009**, *54*, 7201.
16. Bian L. Y., Wang Y. H., Zang J. B., Yu J. K., Huang H.: *J. Electroanal. Chem.* **2010**, *644*, 85.
17. Sivakumar C.: *Electrochim. Acta* **2007**, *52*, 4182.
18. Spataru T., Marcu M., Banu A., Roman E., Spataru N.: *Electrochim. Acta* **2009**, *54*, 3316.
19. Zeng D. M., Jiang Y. X., Zhou Z. Y., Su Z. F., Sun S. G.: *Electrochim. Acta* **2010**, *55*, 2065.
20. Zhang L., Jiang X.: *J. Electroanal. Chem.* **2005**, *583*, 292.
21. Nirmala Grace A., Pandian K.: *Electrochim. Commun.* **2006**, *8*, 1340.
22. Karnicka K., Chojak M., Miecznikowski K., Skunik M., Baranowska B., Kolary A., Piranska A., Palys B., Adamczyk L., Kulesza P. J.: *Bioelectrochemistry* **2005**, *66*, 79.
23. Senthil Kumar S., Mathiyarasu J., Lakshminarasimha Phani K.: *J. Electroanal. Chem.* **2005**, *578*, 95.
24. Manesh K. M., Santhosh P., Gopalan A., Lee K. P.: *Talanta* **2008**, *75*, 1307.
25. Sundfors F., Bobacka J.: *J. Electroanal. Chem.* **2004**, *572*, 309.
26. Pigani L., Heras A., Colina A., Seeber R., Lopez-Palacios J.: *Electrochim. Commun.* **2004**, *6*, 1192.
27. Hass R., Garcia-Canadas J., Garcia-Belmonte G.: *J. Electroanal. Chem.* **2005**, *577*, 99.
28. Zykwińska A., Domagala W., Pilawa B., Lapkowski M.: *Electrochim. Acta* **2005**, *50*, 1625.
29. Melato A. I., Viana A. S., Abrantes L. M.: *Electrochim. Acta* **2008**, *54*, 590.
30. Chen L., Yuan C., Dou H., Gao B., Chen S., Zhang X.: *Electrochim. Acta* **2009**, *54*, 2335.
31. Lupu S.: *Synth. Met.* **2011**, *161*, 384.
32. Lupu S., Totir N.: *Collect. Czech. Chem. Commun.* **2010**, *75*, 835.
33. Bard A. J., Faulkner L. R.: *Electrochemical Methods*, Chaps 3 and 9. Wiley, New York 1980.
34. Sundfors F., Bobacka J., Ivaska A., Lewenstam A.: *Electrochim. Acta* **2002**, *47*, 2245.
35. Koster O., Schuhmann W., Vogt H., Mokwa W.: *Sens. Actuators, B* **2001**, *76*, 573.
36. Bobacka J., Lewenstam A., Ivaska A.: *J. Electroanal. Chem.* **2000**, *489*, 17.
37. Bobacka J., Grzeszczuk M., Ivaska A.: *J. Electroanal. Chem.* **1997**, *427*, 63.
38. Sundfors F., Bobacka J.: *J. Electroanal. Chem.* **2004**, *572*, 309.